

RESEARCH

Open Access



# *Panax quinquefolius* saponins combined with dual antiplatelet therapy enhanced platelet inhibition with alleviated gastric injury via regulating eicosanoids metabolism

Wenting Wang<sup>1,2†</sup>, Lei Song<sup>1,3†</sup>, Lin Yang<sup>1,3</sup>, Changkun Li<sup>4</sup>, Yan Ma<sup>5</sup>, Mei Xue<sup>1,3\*</sup> and Dazhuo Shi<sup>1,3\*</sup>

## Abstract

**Background** *Panax quinquefolius* saponin (PQS) was shown beneficial against platelet adhesion and for gastroprotection. This study aimed to investigate the integrated efficacy of PQS with dual antiplatelet therapy (DAPT) on platelet aggregation, myocardial infarction (MI) expansion and gastric injury in a rat model of acute MI (AMI) and to explore the mechanism regarding arachidonic acid (AA)-derived eicosanoids metabolism.

**Methods** Wistar rats were subjected to left coronary artery occlusion to induce AMI model followed by treatment with DAPT, PQS or the combined therapy. Platelet aggregation was measured by light transmission aggregometry. Infarct size, myocardial histopathology was evaluated by TTC and H&E staining, respectively. Gastric mucosal injury was examined by scanning electron microscope (SEM). A comprehensive eicosanoids profile in plasma and gastric mucosa was characterized by liquid chromatography-mass spectrometer-based lipidomic analysis.

**Results** PQS+DAPT further decreased platelet aggregation, lessened infarction and attenuated cardiac injury compared with DAPT. Plasma lipidomic analysis revealed significantly increased synthesis of epoxyeicosatrienoic acid (EET) and prostaglandin (PG) I<sub>2</sub> (potent inhibitors for platelet adhesion and aggregation) while markedly decreased thromboxane (TX) A<sub>2</sub> (an agonist for platelet activation and thrombosis) by PQS+DAPT, relative to DAPT. DAPT induced overt gastric mucosal damage, which was attenuated by PQS co-administration. Mucosal gastroprotective PGs (PGE<sub>2</sub>, PGD<sub>2</sub> and PGI<sub>2</sub>) were consistently increased after supplementation of PQS+DAPT.

**Conclusions** Collectively, PQS+DAPT showed synergistic effect in platelet inhibition with ameliorated MI expansion partially through upregulation of AA/EET and AA/PGI<sub>2</sub> synthesis while suppression of AA/TXA<sub>2</sub> metabolism. PQS attenuated DAPT-induced gastric injury, which was mechanistically linked to increased mucosal PG production.

**Keywords** *Panax quinquefolius* saponins, Dual antiplatelet therapy, Platelet inhibition, Gastric injury, Lipidomics, Eicosanoids

<sup>†</sup>Wenting Wang and Lei Song are co-first authors.

\*Correspondence:

Mei Xue

[meiar@126.com](mailto:meiar@126.com)

Dazhuo Shi

[shidztc@163.com](mailto:shidztc@163.com)

Full list of author information is available at the end of the article



## Background

Irregulated platelet activation plays a crucial role in atherothrombosis. Dual antiplatelet therapy (DAPT) with aspirin (ASA) and clopidogrel (CLP) is the mainstay of secondary prevention in the setting of acute coronary syndromes (ACS) [1]. However, a considerable number of patients exhibit insufficient platelet inhibition despite DAPT [2–4], which has been associated with a higher risk for atherothrombotic events, such as stent thrombosis and myocardial infarction (MI) expansion [5, 6]. ASA induces a wide spectrum of gastrointestinal (GI) complications, ranging from mucosal erosion, ulcer to severe bleeding [7], which may have an adverse impact on prognosis [8]. DAPT poses significantly increased risks of GI injury compared with ASA alone [9]. Therefore, more effective antiplatelet strategies with limited GI toxicity are much needed.

*Panax quinquefolius* (PQ), commonly known as North American ginseng, possesses a wide range of biological effects and has been extensively employed in Asian societies, particularly in the cardiovascular system [10]. *Panax quinquefolius* saponins (PQS), major bioactive component of stem and leaves of PQ, is a patent Chinese herbal medicine approved by National Medical Products Administration (commercial name as Xinyue capsule, Z20030073) for the treatment of coronary artery disease. The pharmacological actions of PQS have been generally ascribed to multiple triterpenoid ginsenosides (Rb1, Rb2, Rc, Rd, Re and Rg1) as evidenced by high-performance liquid chromatography ultraviolet analysis [11]. We previously revealed that PQS combined with DAPT significantly improved inhibitory effect on platelet adhesion to injured human umbilical vein endothelial cells (HUVECs) [12], an initial phase of platelet activation and thrombosis [13]. Additionally, PQS was shown beneficial for reducing DAPT-related gastric injury in vivo [14]. The joint actions of PQS+DAPT were achieved through unresolved mechanisms that may involve regulation of arachidonic acid (AA) pathway.

Eicosanoids arise from the oxidation of AA and other 20 carbon chain polyunsaturated fatty acids by cyclooxygenase (COX), lipoxygenase (LOX), cytochrome P450 (CYP) enzymes, or via nonenzymatic mechanism. Eicosanoids are highly bioactive oxylipins acting on many cell types and exert multitudinous functions in the cardiovascular, renal and GI systems [15]. Specifically, AA-derived eicosanoids have been found to exhibit anti- or pro-thrombotic activity via regulating platelet and endothelial functions [16]. Additionally, the crucial roles of AA-derived eicosanoids in GI mucosal defense, as well as in GI injury, have also been extensively reported [17, 18]. In our previous in vitro study, the more potent anti-adhesion effect of PQS+DAPT, compared with DAPT, was

mechanically linked to enhanced synthesis of endothelial prostaglandin (PG) I<sub>2</sub> [12], an AA/COX downstream eicosanoid with potent antiplatelet action [19]. Interestingly, ameliorated gastric injury by adding PQS to DAPT was associated with AA/COX/PGE<sub>2</sub> pathway [14]. These results suggested a regulatory role of PQS in AA-derived eicosanoids metabolism, which warrant further investigations.

In the present study, we examined the integrated efficacy of PQS combined with DAPT on platelet inhibition, MI expansion and gastric injury in a rat model of acute MI (AMI). The emerging field of pharmacometabolomics, including lipidomics, have contributed to understanding the mechanism of drug actions through identification of metabolic signatures associated with therapeutic responses [20]. Mechanistically, we conducted an AA-targeted lipidomic analysis of eicosanoids metabolic alterations in response to PQS+DAPT, relative to DAPT, in rat plasma and gastric mucosa.

## Methods

### Drugs and reagents

PQS (commercial name as Xinyue capsules, 50 mg PQS/capsule, National medicine permit No. Z20030072) was provided by Yisheng Pharmaceutical Co., Ltd (Jilin, China, batch No.180102). PQS was shown consistent quality between different batches and six ginsenosides (Rb1, Rb2, Rc, Rd, Re and Rg1) were detected as the major active compounds of PQS by our previous high-performance liquid chromatography ultraviolet analysis (the chemical structure of these ginsenosides were shown in Fig. S1) [11]. ASA was purchased from BAYER (Beijing, China). CLP was purchased from Sanofi (Paris, France). Adenosine diphosphate (ADP) were purchased from Chrono-log Corporation (Havertown, Pennsylvania, USA). 2,3,5-triphenyltetrazolium chloride (TTC) was purchased from Sigma-Aldrich (St. Louis, MO, USA). Internal standards for lipidomics analysis including 6-keto-PGF1 $\alpha$ -d4, Thromboxane (TX) B<sub>2</sub>-d4, PGF2 $\alpha$ -d4, PGE<sub>2</sub>-d4, PGD<sub>2</sub>-d4, Leukotriene (LT) C<sub>4</sub>-d5, LTB<sub>4</sub> d4, 15-hydroxyeicosatetraenoic acid (HETE) -d8, 12-HETE-d8, 5-HETE -d8, AA-d8 were purchased from Cayman Chemical (Ann Arbor, Michigan, USA). The liquid chromatography-mass spectrometer (LC-MS)-grade solvents, methyl alcohol, acetonitrile, formic acid and ethanol were purchased from Thermo Fisher Scientific (Waltham, Massachusetts, USA).

### Animals and ethic

All animal protocols were approved by the Xiyuan Hospital Institutional Animal Care and Use Committee and performed in accordance with the national guidelines for the care and use of laboratory animals

issued by Ministry of Science and Technology of the People's Republic of China. This study was reported in accordance with ARRIVE (Animal Research: Reporting of In Vivo Experiments) guidelines. Male Wistar rats (weighted between 180 and 210 g) were purchased from Beijing University Laboratory Animal Center (Beijing, China; certificate number SCXK [Jing] 2011-0004). Rats were allowed to acclimatize under standard care conditions for at least 7 days.

#### AMI model and experimental design

AMI was induced by permanent ligation of left anterior descending (LAD) coronary artery as described previously [21]. At the onset of ligation, rats were weighted between 220 and 250 g. AMI rats were randomized into 4 groups: AMI group, PQS group, DAPT group and PQS+DAPT group ( $n=12$  for each group). Another group of rats were subjected to the same operation except for ligation (sham group,  $n=12$ ). From day one to day twenty-nine after surgery, rats in drug intervention groups were administered daily by oral gavage with PQS at dose of 27 mg/kg, or ASA at loading dose of 27 mg/kg (for only 1 day) and then maintenance dose of 9 mg/kg combined with CLP at loading dose of 27 mg/kg (for only 1 day) and then maintenance dose of 6.75 mg/kg, or PQS added to DAPT, respectively. Rat PQS dosage was 257 mg/ Kg, which was equivalent to 42.85 mg/ Kg daily for humans as manual recommended. Loading and maintenance dosage of DAPT for rats were converted in accordance with human guideline recommendations [1]. For rats in sham and AMI group, same volume of physiological saline was orally administered.

Twenty-four hours after last medication, rats were euthanized under anesthesia (pentobarbital sodium, 30 mg/kg, IP) for exsanguination by abdominal aorta puncture. Whole blood drawn from abdominal aorta were collect in vacutainer tubes containing 3.8% trisodium citrate [22] and EDTA [23] for platelet aggregatory assay and lipidomic analysis, respectively. Hearts were harvested and maintained at  $-80^{\circ}\text{C}$  for fur-

tissues taken from antrum were used for ultrastructure scanning and lipidomic characterization.

#### Measurement of platelet aggregation

Platelet aggregation was measured by light transmission aggregometry assay in a 8-channel aggregometer (Pulisheng Instrument Co. Ltd., Shanghai, China) as previously described [25]. 3.8% trisodium citrate-anticoagulated whole blood was centrifuged ( $260\times\text{g}$ , 10 min) to obtain platelet-rich plasma (PRP). The remaining blood was further centrifuged ( $760\times\text{g}$ , 10 min) to obtain platelet-poor plasma (PPP). PRP was adjusted to platelet counts of  $1\times 10^8/\text{mL}$  with PPP. Before agonist stimulation, light transmission was adjusted to 100% with PPP and to 0% with PRP. After preincubation with ADP at final concentration of 10  $\mu\text{mol/L}$ , aggregation curve was recorded over 5 min (with 100% aggregation corresponding to 100% light transmission). Maximal platelet aggregation was calculated as percent change in light transmission.

#### Myocardial histopathology

Myocardial issue specimens were fixed in 10% formaldehyde and embedded in paraffin. The waxes were sectioned at 5- $\mu\text{m}$  thickness and then deparaffinized and rehydrated. Standard H&E staining was carried out for histopathological examinations. Myocardium structure was observed under a microscope (Olympus, Tokyo, Japan) and analyzed by Image-pro plus 6.0 (Media Cybernetics, Maryland, USA).

#### Infarct size quantification

The myocardial infarct size was evaluated by TTC staining as previously described [26]. Briefly, the frozen heart was sectioned into 5 slices along the left ventricle (LV) long axis and stained with 0.25% TTC at  $37^{\circ}\text{C}$  for 30 min in the dark. The stained heart slices were photographed with a digital camera. The infarct size was visualized using Image J (Bethesda, MD, United States) and quantified according to the equation:

$$[\text{infarct area of LV}/(\text{cross - sectional area of LV} - \text{area of LV chamber})] \times 100\%$$

ther analysis. One cohort ( $n=10$  for each group) was stained by TTC for infarct volume quantification and the other cohort ( $n=2$  for each group) was subjected to hematoxylin and eosin (H&E) staining for myocardium histopathological examination. Evidence from clinical observations suggests that patients on antiplatelet treatment develop endoscopic-confirmed gastric lesions more frequently in the antrum [24]. Mucosal

#### Observation of gastric mucosal injury

Gastric antrum mucosal samples ( $40\times 10\times 10$  mm block) were pre-fixed with 2.5% glutaraldehyde ( $\text{pH}=7.2$ ) at room temperature for 3 days followed by post-fixation with 1% osmium for 2 h at room temperature. Samples were dehydrated in ascending grades of ethanol (30%, 40%, 50%, 60%, 70%, 80%, 90%, 95%, 100%, each for 10 min). Samples were critical point dried and coated

with gold palladium. The ultrastructure of gastric mucosa was imaged with a scanning electron microscope (SEM) (HITACHI, Japan) operating at 10 kV.

### Lipidomic analysis

#### Sample preparation and lipid extraction

AA-derived eicosanoids were extracted according to the procedure described previously [27]. EDTA-anticoagulated whole blood was centrifuged (2000×g, 15 min, 4 °C) and plasma was collected. Internal standards were added into 50 mg of gastric mucosa and 600 µL plasma samples at the final concentration of 83 ng/mL (except for AA-d8 of 166 ng/mL). Samples were then vortexed for 3 min. After centrifugation (4000×g, 5 min, 4 °C), the upper layer (550 µL of gastric mucosal sample and 1 mL of plasma) was supplemented with 4 mL 0.1% formic acid and vortexed for 30 s. Then samples were placed into a preconditioned solid phase extraction cartridge (Phenomenex, 10 mg/mL, California, United States) and washed with 0.1% formic acid and 15% ethyl alcohol. After elution with methanol, lipid extract was evaporated and stored at -80 °C prior to lipidomic analysis.

#### LC-MS-based lipid profiling

The lipid extract was reconstituted in 100 µL methanol and vortexed for 5 min. After centrifuged (12,000×g, 6 min, 4 °C), 80 µL of supernatant was transferred to a vial insert for analysis. AA-targeted lipid profiling was performed with a modified LC-MS methodology (LCMS-8050, Shimadzu, Kyoto, Japan) as previously reported [28]. LC-MS data were acquired using multiple-reaction monitoring mode with continuous ionization polarity switching. Chromatographic separation was achieved using a Phenomenex Kinetex C8 column (150×2.1 mm inner diameter, 2.6 µm film thickness). Mobile phase solutions were 0.1% formic acid for A and acetonitrile for B. The flow rate was maintained at 0.4 mL/min with the column temperature set to 40 °C. The solvent gradient was applied as follows: starting at 10% B and increasing to 25% B over 5 min, then to 35% B over 5 min, to 75% B over 10 min, to 95% B over 0.1 min, then held at 95% B for 4.9 min and returned to 10% B over 0.1 min. The injection volume was 5 µL for each run. The ionization was done in both positive and negative mode. Mass spectrometer running conditions were as follows: drying gas flow rate 15 L/min, heating gas flow rate 10 L/min, nebulizing gas flow rate 3 L/min, collision gas (argon gas, purity >99.9995%) voltage 270 kPa, heat block temperature 400 °C, ESI interface temperature 300 °C, desolvation line temperature 250 °C.

#### Data processing and multivariate analyses

LC/MS raw data were assessed with LabSolutions (version 5.86, Shimadzu, Kyoto, Japan) for lipid identification,

peak extraction, peak alignment, noise filtering and data extraction. Lipid response was calculated as the peak area ratio of the target analyte to the respective internal standard [29]. Then data were log-transformed for multivariate statistical analysis by SIMCA-P 14.1 (Umeta, Umeå, Sweden) and back-transformed for presentation as median (interquartile range) [29]. After auto-scaling, data were subjected to principal component analysis (PCA) to visualize the differences of lipid profile between DAPT and PQS+DAPT group. Orthogonal projection to latent structure-discriminant analysis (OPLS-DA) was further used to validate the lipidomic alterations by adding PQS to DAPT. The robustness of OPLS-DA model was validated by permutation testing. Lipid biomarkers that significantly differentiated between DAPT and PQS+DAPT group were determined based on the combinational thresholds of variable importance in projection (VIP) values larger than 1.0 obtained from OPLS-DA model and *P* values less than 0.05 obtained from Mann-Whitney *U* test.

### Statistical analyses

Statistics except of lipidomic analysis were performed using SPSS (version 21.0, Chicago, Illinois, USA). Normally distributed variables were presented as mean ± SEM. For multiple group comparisons, one-way ANOVA was performed with LSD as post hoc correction. Differences were considered statistically significant at *P* < 0.05.

## Results

### PQS+DAPT enhanced inhibitory effect on platelet aggregation

Platelet activation and thrombus formation is a multistage process including shape change, platelet adhesion and aggregation [30]. We previously revealed more potent inhibition of platelet adhesion to oxidized low-density lipoprotein injured HUVEC by PAS+DAPT compared with DAPT [12]. The present study further studied the anti-aggregatory effect of the joint therapy in a rat model of AMI. Platelet aggregation was analyzed in citrate-anticoagulated PRP to avoid agonists released from erythrocytes [31]. At 29 days after surgery, maximum platelet aggregation rate (MPAR) induced by ADP increased markedly in AMI rats compared with those with sham operation, indicating enhanced platelet reactivity post MI (*P* < 0.01, Fig. 1A). Rat treated with PQS alone and in combination with DAPT showed significantly decreased MPAR compared with those in AMI group (both *P* < 0.01, Fig. 1A). Furthermore, PQS+DAPT decreased MPAR compared with DAPT (*P* < 0.05, Fig. 1A), suggesting a reinforced anti-aggregatory effect of the combined therapy.

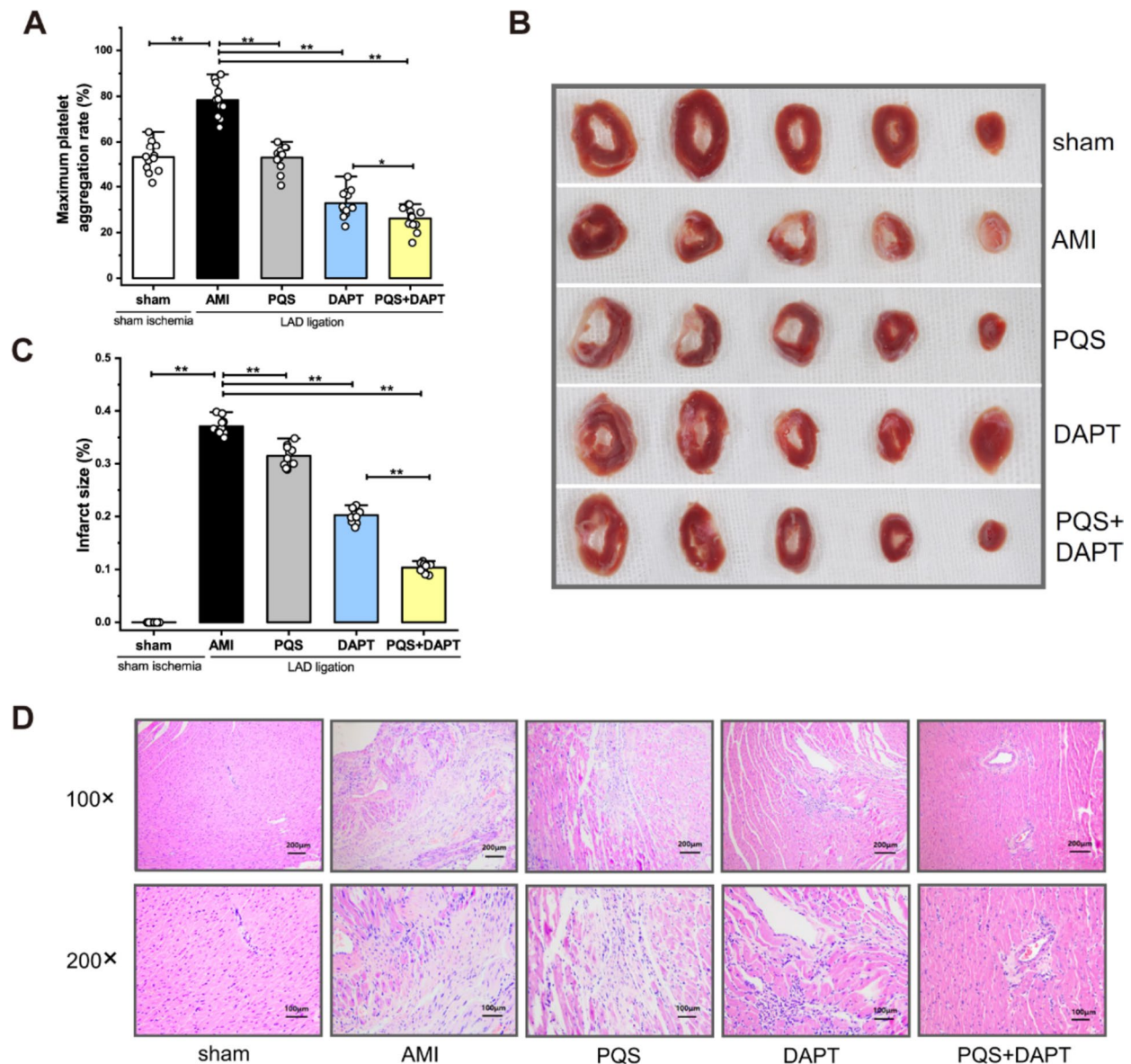


**Fig. 1** PQS+DAPT further decreased platelet aggregation, attenuated MI expansion and cardiac injury in AMI rats. **A** ADP-induced MPA measured by light transmission aggregometry revealed potentiated inhibition of platelet aggregation by PQS+DAPT compared with DAPT. Each dot represents one rat ( $n = 12$ ). **B** MI expansion was visualized by TTC staining and infarct size was measured using Image J software. PQS+DAPT further diminished infarct size relative to DAPT. Each dot represents one rat ( $n = 10$ ). **C** Representative images of TTC staining. **D** Representative images of myocardial histopathology by H&E staining ( $\times 100$ , Scale bar: 200  $\mu\text{m}$ ;  $\times 200$ , Scale bar: 100  $\mu\text{m}$ ). Multiple group comparison was conducted by one-way ANOVA.  $*P < 0.05$ ,  $**P < 0.01$ . Data were mean  $\pm$  SEM in all panels

### PQS+DAT ameliorated MI expansion

Irregular platelet activation may induce thrombotic occlusion of vessel lumen, leading to myocardial infarction expansion [32]. While platelet adhesion represents the initial phase of thrombosis, platelet aggregation is the key step of platelet accumulation amplifying thrombus formation [13]. We next addressed the impact of PQS, DAPT or the combined therapy on infarct size. Rats subjected to permanent

occlusion of LAD coronary artery exhibited transmural infarction, as shown in Fig. 1B. PQS monotherapy, DAPT and PQS+DAPT suppressed MI expansion post MI (both  $P < 0.01$  vs AMI rats, Fig. 1C), with a significantly reduced infarct size in response to PQS+DAPT compared with DAPT ( $P < 0.01$ , Fig. 1C). Thus, these findings indicated that adding PQS to DAPT achieved greater platelet inhibition and further ameliorated MI progression.

### PQS+DAPT alleviated cardiac injury

To determine the influence of PQS, DAPT or the combined therapy on myocardial histopathology, H&E staining was performed (Fig. 1D). Rats subjected to sham surgery exhibited normal myocardial structural patterns. Hearts of AMI rats exhibited significant morphologic changes at 30 days post-MI, showing massive dense collagenous scar with a few vital myocytes. In PQS-treated rats, areas of cardiac damage were slightly diminished, characterized with narrowed collagen deposition and increased cellularity. DAPT significantly reduced the extent of myocardial necrosis with limited scar formation. Intriguingly, adding PQS to DAPT further lessen the size of infarct and markedly alleviated the degree of cardiac injury.

### PQS mitigated DAPT-induced gastric mucosal injury

It has been reported that ultrastructural damage to the gastric epithelium occurs during short-term administration of ASA with no area of the stomach resistant to the injury. The most frequently and severely affected site is the gastric antrum [33]. In the present study, antrum specimen was collected for better observation of the gastric injury. Rats treated with saline and PQS exhibited normal cobblestone structure with regular arrangement of epithelial cells (Fig. 2A-C). After DAPT administration, overt epithelium deformation was observed. Moreover, DAPT caused a vast ablation of the surface epithelium; thereby, the honeycomb structure of the denuded lamina propria became apparent (Fig. 2D). By contrast, gastric mucosa in PQS+DAPT-treated rats showed a few apical erosions while the severity of surface desquamation was diminished (Fig. 2E), indicating alleviated gastric injury by adding PQS to DAPT.

### AA-targeted lipidomic analysis revealed alteration of eicosanoids metabolism in plasma by adding PQS to DAPT

AA-derived eicosanoids produced by platelets and endothelial cells exert expansive role on platelet biology that significantly regulate platelet reactivity [16]. They can be secreted by cells and stable metabolites may accumulate in circulation. To determine the impact of PQS+DAPT, relative to DAPT, on eicosanoids profile in plasma, a robust LC-MS-based, AA-targeted lipidomic profiling was performed after 30 days of drug intervention. The platform determined 87 AA-derived lipids including eicosanoids and breakdown products, among which 37 were detectable in plasma (Fig. 3 and Table S1). The preprocessed LC/MS data were subjected to PCA analysis and samples with similar lipid profiles were clustered closely in the score plot of PCA. As shown in Fig. 4A, distinct clusters for plasma lipid profile in DAPT and PQS+DAPT group was observed, suggesting alteration of eicosanoids metabolism by adding PQS to DAPT. Supervised OPLS-DA analysis further confirmed the metabolic differences between DAPT and PQS+DAPT groups (Fig. 4B). The robustness of PLS-DA model was validated by 200-repeated permutation test (Fig. 4C). The heatmap provided a metabolic snapshot of the plasma lipid profile (Fig. 4D). Thirteen lipids with VIP value higher than 1.0 were considered potential pharmacological biomarkers in response to PQS+DAPT compared with DAPT (Table S2).

To figure out lipids that were significantly up-/ down-regulated by PQS+DAPT compared with DAPT, Mann-Whitney *U* test was used. 9 out of 13 lipids remained significantly differentiated between the two groups (Fig. 5A-D, Table S3, and receiver operating characteristic analysis for these 9 lipids between DAPT group and PQS+DAPT group were shown in Fig. S2A-D).

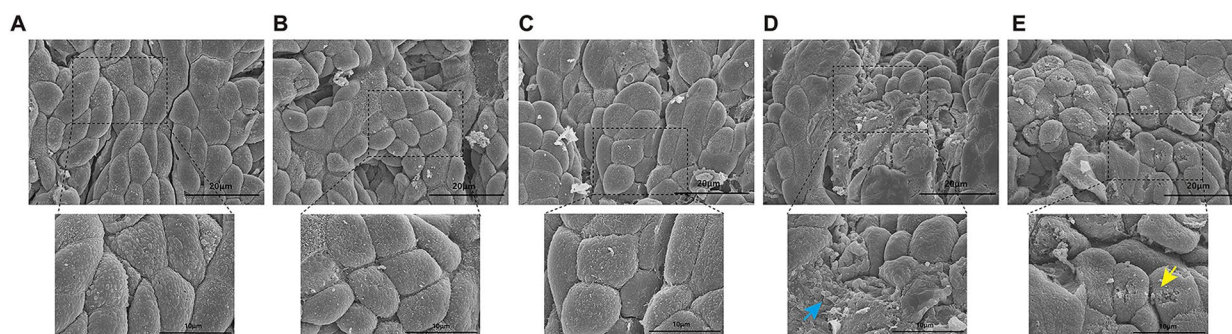


**Fig. 2** PQS mitigated DAPT-induced gastric mucosal injury. Representative images of gastric antrum mucosa by SEM in **A** sham group, **B** AMI group, **C** PQS group, **D** DAPT group and **E** PQS+DAPT group. ( $\times 5000$ , Scale bar: 10  $\mu\text{m}$ ; insert image  $\times 2000$ , Scale bar: 20  $\mu\text{m}$ ). DAPT caused a vast ablation of the gastric surface epithelium (shown in blue arrow). In PQS+DAPT treated rats, mucosa injury was attenuated, as demonstrated by a few apical erosions (shown in yellow arrows)

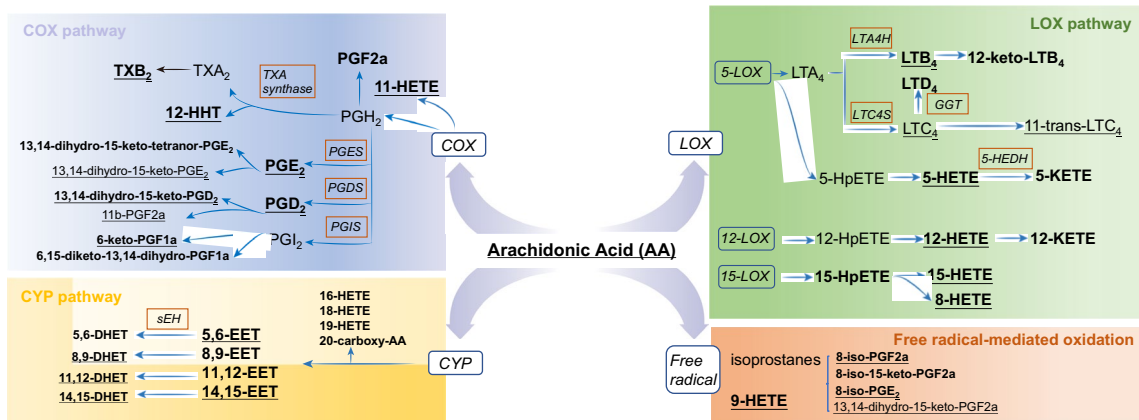


**Fig. 3** Eicosanoid biosynthesis from AA via COX, LOX, CYP enzymatic pathways as well as by free radical-mediated oxidation. COX, LOX, CYP are shown in blue ovals and downstream enzymes are shown in red boxes. Note that eicosanoid detected in plasma are in bold and those detected in mucosa are underlined

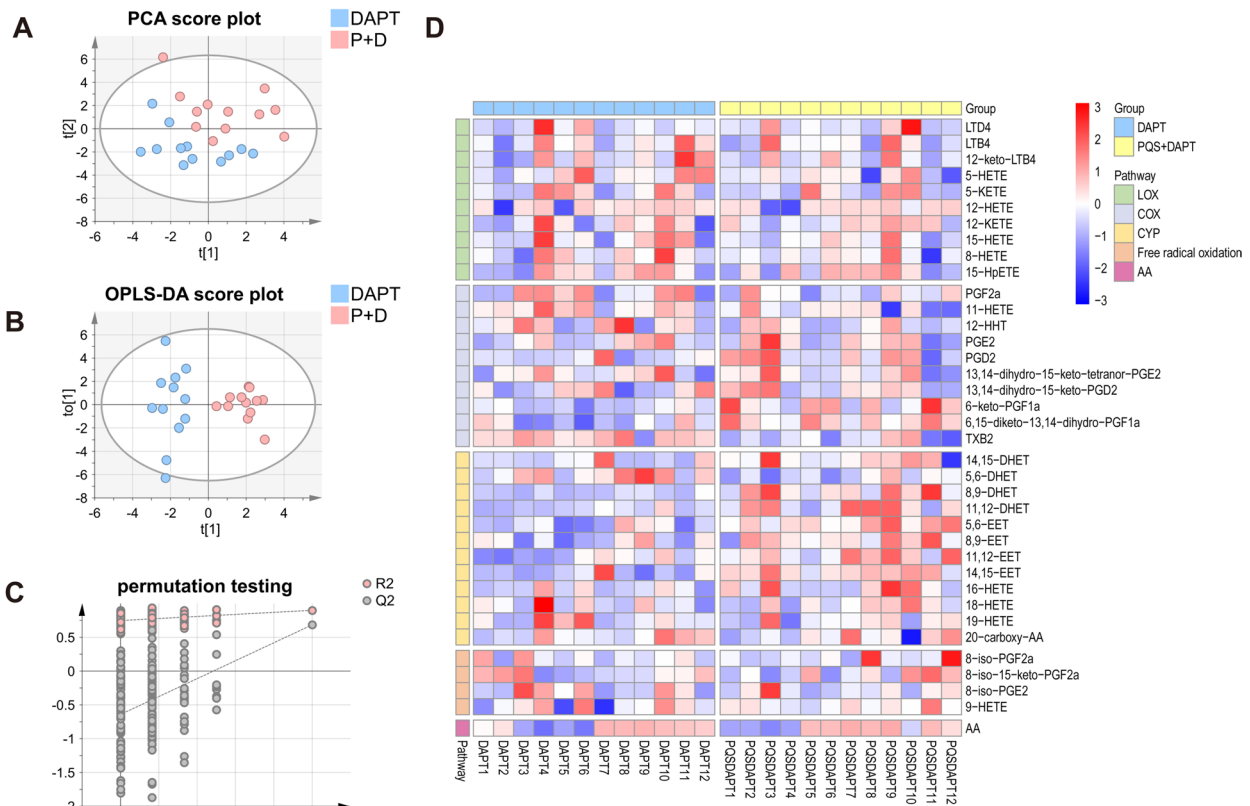


**Fig. 4** Lipidomic analysis for plasma unraveled significantly altered eicosanoids profile by adding PQS to DAPT. Multivariate analysis results shown in **A** PCA score plot and **B** OPLS-DA score plot demonstrated distinct discrimination of plasma lipid profile in DAPT group compared with PQS+DAPT group. **C** Validation of OPLS-DA model by permutation testing. **D** Heatmap analysis provided a metabolic snapshot of the plasma lipid profile in the two groups. P+D, PQS+DAPT

Specifically, there were significant increases in the abundance of epoxyeicosatrienoic acids (EETs) (5,6-EET, 8,9-EET, 11,12-EET, 14-15-EET) and downstream

dihydroxyeicosatrienoic acids (DHETs) (8,9-DHET, 11-12DHET), all from CYP pathway, in PQS+DAPT group as compared to DAPT group (Fig. 5A-B).

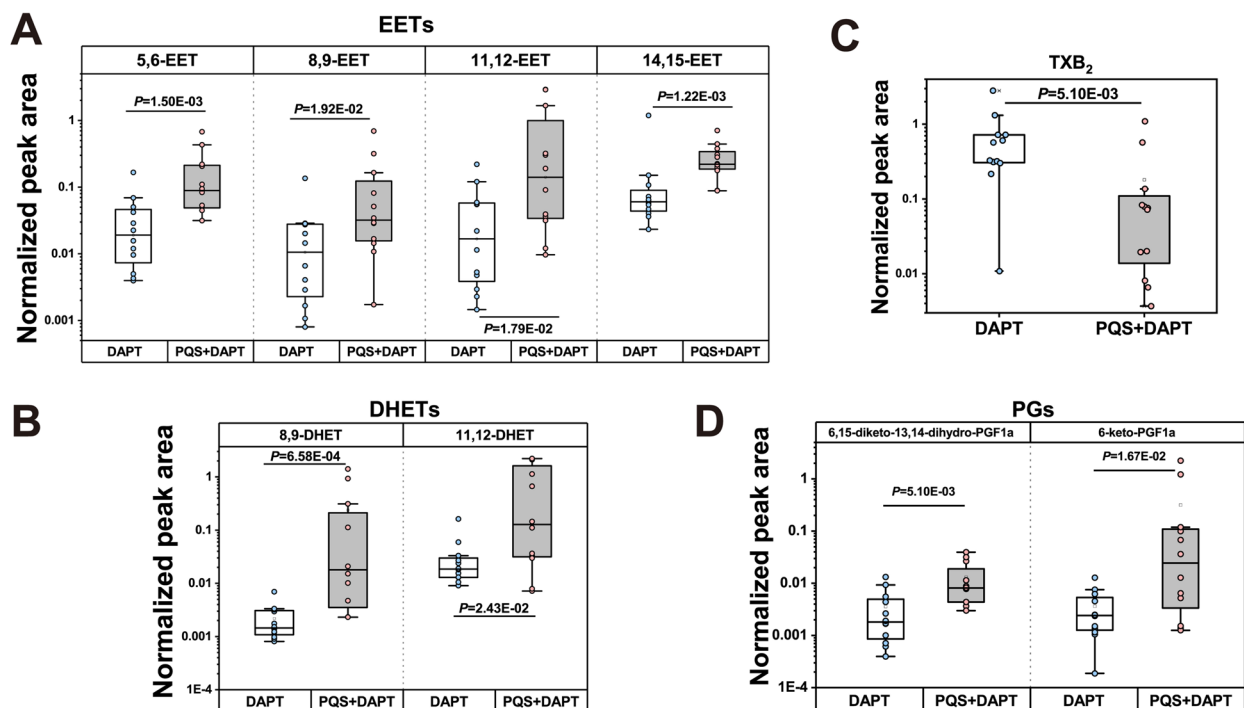


**Fig. 5** Lipidomic analysis unraveled significantly altered plasma eicosanoids by adding PQS to DAPT. Plasma level of **A** EETs, **B** DHETs, **C** TXB<sub>2</sub> and **D** PGI<sub>2</sub> downstream lipids were shown in box plots. Each dot represents one rat ( $n = 12$ ). Data were presented as median (interquartile range) in all panels

Moreover, PQS supplementation to DAPT resulted in a roughly 6-fold decrease in plasma level of thromboxane (TX)B<sub>2</sub>, while led to significantly up-regulation of 6-keto-PGF1a and 6,15-diketo-13,14-dihydro-PGF1a, downstream metabolites of PGI<sub>2</sub> (Fig. 5C-D).

#### AA-targeted lipidomic analysis uncovered alteration of eicosanoids metabolism in gastric mucosa by adding PQS to DAPT

AA-derived eicosanoids in gastric lumen are locally acting bioactive lipids that play homeostatic roles ranging from regulating vascular leakage, barrier formation to protecting mucosal integrity [34]. We harvested gastric mucosa from antrum, the most vulnerable site to ASA-related GI toxicity, to investigate mucosal lipidomic alteration in response to PQS+DAPT, relative to DAPT. A total of 26 lipids were identified in antrum mucosa by LC/MS analysis as shown in Fig. 3 and Table S4. Score plot of PCA analysis revealed separated clusters for gastric lipid profile in DAPT and PQS+DAPT group with partly overlapping 95% confidence intervals, indicating that gastric lipidomic profile was altered by adding PQS to DAPT (Fig. 6A). Next, OPLS-DA analysis was conducted and validated as shown in Fig. 6B-C. Score plot of OPLS-DA model demonstrated more clear classification of lipid

profile in the two groups. Heatmap analysis visualized the gastric lipid profile in both groups, suggesting up-regulated synthesis of lipids downstream of AA/COX pathway in response to PQS+DAPT, relative to DAPT (Fig. 6D). As Expected, 7 lipids with VIP higher than 1.0 were all derived from AA/COX pathway (Table S5).

Six out of 7 lipids reached statistical significance by Mann-Whitney  $U$  test, reflecting the eicosanoids significantly changed by PQS+DAPT treatment compared with DAPT (Fig. 7A-F, Table S6, and receiver operating characteristic analysis for these 6 lipids between DAPT group and PQS+DAPT group were shown in Fig. S2E-G). Adding PQS to DAPT resulted in approximately 20-fold increase of gastric PGE<sub>2</sub> and its breakdown product 13,14-dihydro-15-keto-PGE<sub>2</sub> relative to DAPT (Fig. 7A-B). Similarly, we observed over tenfold elevation of gastric PGD<sub>2</sub> and 11b-PGF2a, 13,14-dihydro-15-keto-PGD<sub>2</sub>, 6-keto-PGF1a (downstream metabolites of PGD<sub>2</sub> and PGI<sub>2</sub>) in PQS+DAPT group compared with DAPT group (Fig. 7C-F).

#### Discussion

This study demonstrated that adding PQS to DAPT achieved more potent antiplatelet effect with ameliorated MI expansion and cardiac injury in a rat model of AMI. PQS, as an adjunct to DAPT, mitigated



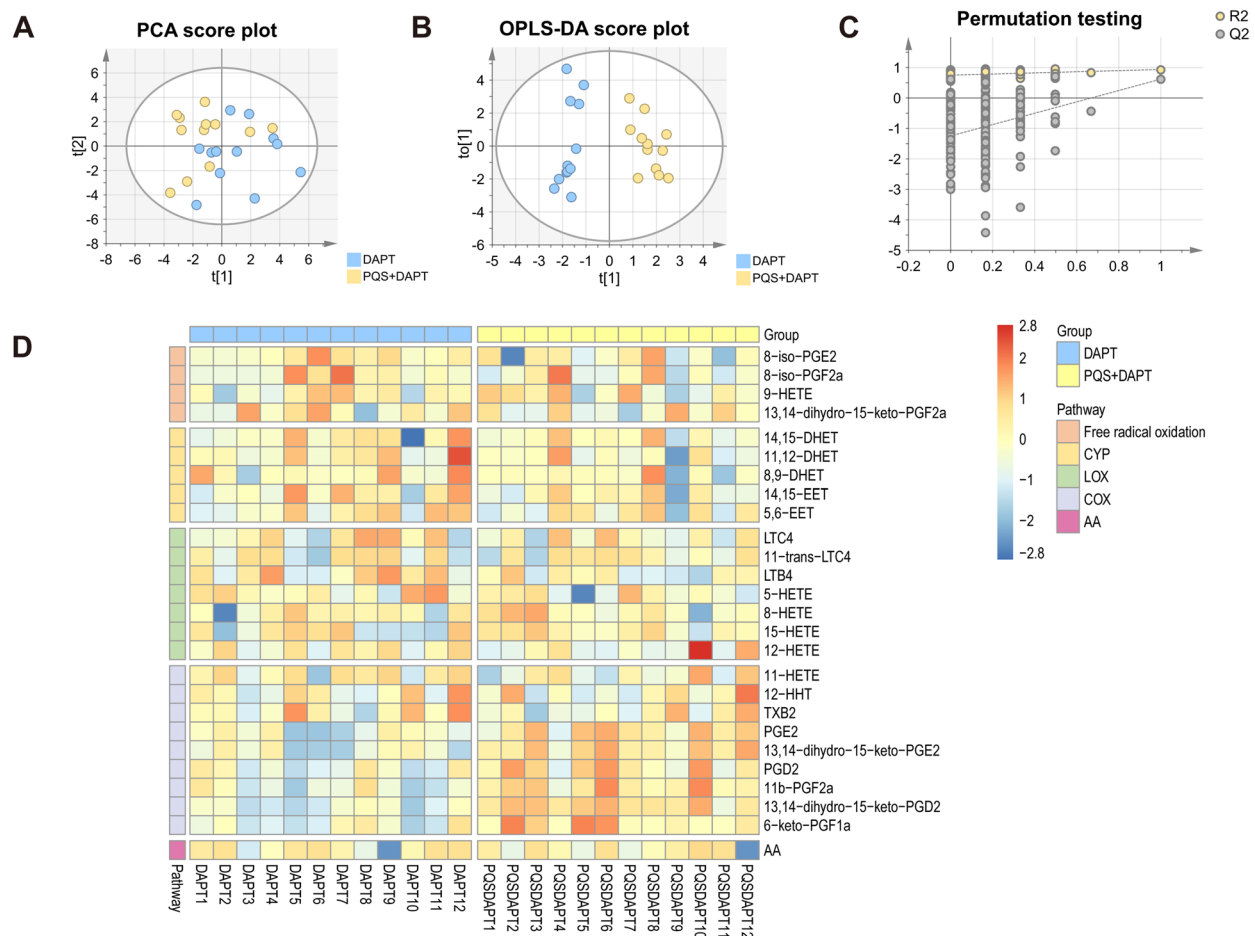


**Fig. 6** Lipidomic analysis for gastric mucosa uncovered significantly altered eicosanoids profile by adding PQS to DAPT. Multivariate analysis results shown in **A** PCA score plot and **B** OPLS-DA score plot demonstrated distinct discrimination of gastric lipid profile in DAPT group compared with PQS+DAPT group. **C** Validation of OPLS-DA model by permutation testing. **D** Heatmap analysis visualized the gastric lipid profile in the two groups

DAPT-related gastric damage illustrated by SEM. By lipidomic approaches, we comprehensively characterized metabolic alterations of AA-derived eicosanoids in response to PQS+DAPT, relative to DAPT, in rat plasma and gastric mucosa. Plasma lipidomic analysis revealed markedly increased EETs, PGI<sub>2</sub>, potent inhibitors of platelet adhesion and aggregation, and significantly decreased TXB<sub>2</sub>, stable form of a potent platelet agonist-TXA<sub>2</sub>, by adding PQS to DAPT, suggesting the improved platelet inhibition of PQS+DAPT may be partly attributed to up-regulated AA/EET, AA/PGI<sub>2</sub> and down-regulated AA/TXA<sub>2</sub> metabolism. Additionally, PQS supplementation to DAPT markedly elevated gastric PGE<sub>2</sub>, PGD<sub>2</sub> and their downstream lipids, which play pivotal roles in mucosal defense. The gastroprotective action of PQS on DAPT-induced gastric injury could be associated with locally augmented PG production in gastric mucosa (Fig. 8).

Suboptimal platelet inhibition despite the use of DAPT has been reported commonly in the setting of ACS [35, 36]. Here, we found a synergistic antiaggregatory effect when adding PQS to DAPT in AMI rats. The benefits of PQS have been generally ascribed to ginsenosides [10], including mainly ginsenoside Rb1, Rb2, Rc, Rd, Re and Rg1. Our finding is in accordance with an earlier in vitro study showing that ginsenoside Rg1 potently inhibited platelet aggregation [37]. Notably, under ischemic stress post MI, uncontrolled platelet activation and aggregation would induce acute vessel occlusion, leading to ongoing MI expansion [38]. Presently, adding PQS to DAPT resulted in significantly reduced MI expansion and alleviated cardiac injury, which was associated with potentiated platelet inhibition. Moreover, inadequate platelet inhibition despite DAPT has been associated with 2-9 fold increased risk of major cardiovascular events [36]. We recently

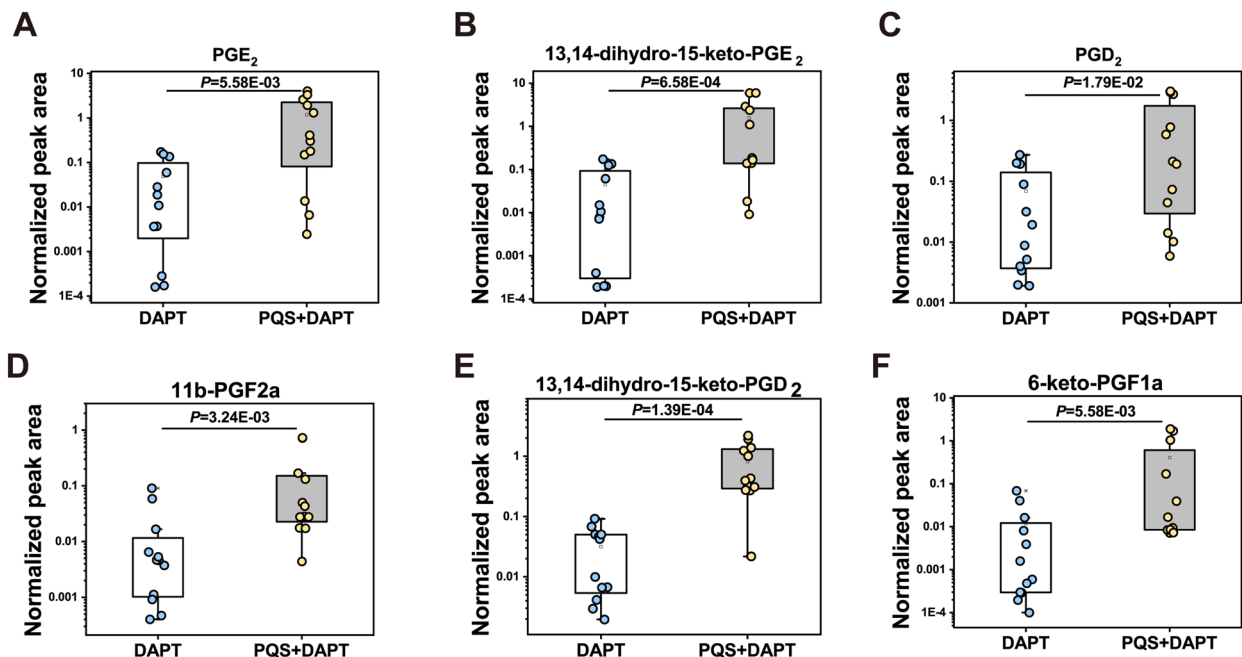


**Fig. 7** Lipidomic analysis unraveled significantly altered gastric eicosanoids by adding PQS to DAPT. Plasma level of **A** PGE<sub>2</sub>, **B** 13,14-dihydro-15-keto-PGE<sub>2</sub>, **C** PGD<sub>2</sub>, **D** 11b-PGF<sub>2a</sub>, **E** 13,14-dihydro-15-keto-PGD<sub>2</sub> and **F** 6-keto-PGF<sub>1a</sub> were shown in box plots. Each dot represents one rat (n = 12). Data were presented as median (interquartile range) in all panels

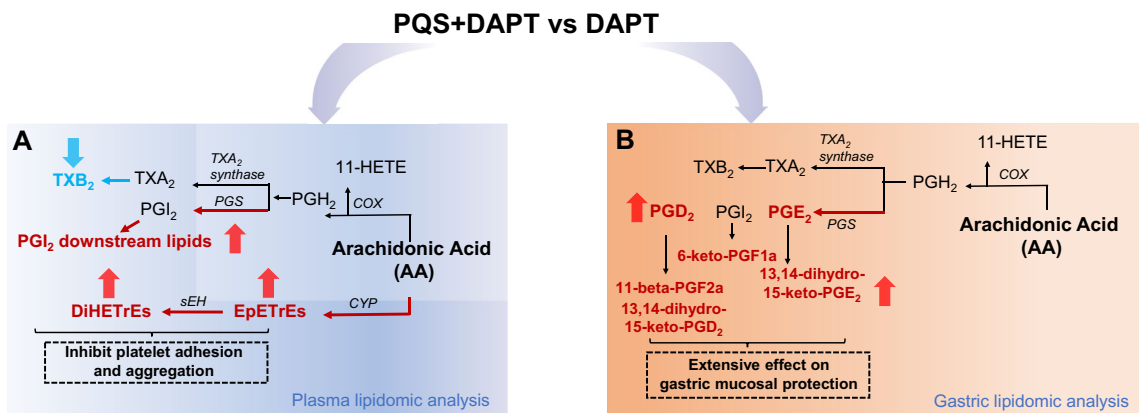


**Fig. 8** Mechanisms underlying the enhanced platelet inhibition and gastroprotection by PQS+DAPT was associated with eicosanoids metabolic modulation. Regulated pathway in **A** plasma and **B** gastric mucosa. The arrows indicated upregulated (red arrows) or downregulated (blue arrows) in PQS+DAPT group relative to DAPT group. Enzymes are illustrated in italics. PGS indicates PG synthase; sEH, soluble epoxide hydrolase

demonstrated that PQS+DAPT further reduced the incidence of primary composite endpoint (cardiac death, nonfatal MI and urgent revascularization) in patients underwent percutaneous coronary intervention [39]. Therefore, these findings suggested that PQS provided incremental benefit in platelet inhibition when added to DAPT, which might contribute to cardiac protection under ischemic conditions.

AA-derived eicosanoids are essential for maintaining vascular homeostasis through actions on platelets

and endothelial cells [16]. Acting as autocrine or paracrine mediators, eicosanoids can be secreted by tissues and stable metabolites will accumulate in plasma [40]. Eicosanoids metabolic patterns are highly sensitive to physiological stimuli including drug interventions [41]. Currently, plasma lipidomic profile provided an accurate snapshot of metabolic alterations after adding PQS to DAPT. We observed significantly increased abundance of CYP-derived EETs and their breakdown metabolites (8,9-DHET, 11-12DHET) resulted from

PQS+DAPT compared with DAPT. EETs are potent vasodilators primarily generated by endothelial cells [42]. Besides, EETs exert anti-inflammatory effects in blood vessels, limiting platelet aggregation [43], which may account for the greater anti-aggregatory effect of PQS+DAPT in the present study. In addition, EETs were shown to cause membrane hyperpolarization of platelets that ultimately suppress platelet adhesion to endothelial cells [44]. Collectively, PQS potentiated DAPT-mediated inhibition of platelet adhesion, as reported previously [12], and aggregation, effects that may partially be ascribed to upregulation of AA/EET metabolism.

Furthermore, the addition of PQS to DAPT augmented synthesis of PGI<sub>2</sub> while decreased production of TXA<sub>2</sub>, as evidenced by a roughly 10-fold increase in plasma 6-keto-PGF<sub>1α</sub>, 3-fold increase in plasma 6,15-diketo-13,14-dihydro-PGF<sub>1α</sub> (PGI<sub>2</sub> downstream metabolites) and a 4-fold decrease in plasma TXB<sub>2</sub> (stable form of TXA<sub>2</sub>). This is consistent with our previous finding that adding PQS to DAPT markedly increased 6-keto-PGF<sub>1α</sub>/TXB<sub>2</sub> ratio in rat plasma [14]. The primary antiplatelet effect of ASA is to acetylate platelet COX-1 and thereby inhibit the synthesis of TXA<sub>2</sub>, a powerful agonist for platelet activation and aggregation [45]. However, insufficient inhibition of TXA<sub>2</sub> biosynthesis despite ASA has been associated with an increased risk of cardiovascular events [46]. The down-regulated TXA<sub>2</sub> metabolism in response to PQS+DAPT may underlie the enhanced anti-aggregatory effect of the integrated therapy, which could also contribute, at least in part, to the reduced cardiovascular events as recently reported [39]. In contrast, PGI<sub>2</sub> counteract the prothrombotic properties of TXA<sub>2</sub> and efficiently inhibits platelet activation [19]. Interestingly, EETs were shown to suppress TXB<sub>2</sub> formation in vivo [47]. Taken together, adding PQS to DAPT reinforced platelet inhibition by maintaining antithrombotic milieu via promoting AA/PGI<sub>2</sub> and AA/EET synthesis while suppressing AA/TXA<sub>2</sub> metabolism.

ASA, even at low doses (75–225 mg/day), is known to cause various GI damage, ranging from mucosal injury to more severe GI bleeding, the latter is independently associated with mortality [8]. Of note, it has been reported that more than 60% of patients taking low dose ASA show endoscopic gastric erosions [48], especially in the gastric antrum [24]. Indeed, ASA-induced gastric injury is substantially more common than overt bleeding and has been considered as a surrogate for the propensity of GI hemorrhagic complications. The addition of CLP to ASA further increases the risk of gastric injury by impairing mucosal healing [49]. Nearly 90% of

DAPT users develop endoscopic gastric mucosal injury [50]. In the present study, gastric antrum tissue was selected for better observation of gastric injury. DAPT causes significant mucosal damage characterized by a vast ablation of epithelium and the exposure of the lamina propria, which was attenuated by PQS administration. Unfortunately, DAPT-related gastric injury is largely asymptomatic [51], rendering suboptimal utilization of gastroprotective regimen. Although guidelines recommend concomitant use of proton pump inhibitors (PPIs) in patients receiving DAPT to reduce GI bleeding [52], PPI has been found to mitigate the anti-aggregatory effect of ASA [53]. In light of the above-mentioned evidence, the pleiotropic effect of PQS on platelet inhibition and gastroprotection suggest it as a potential supplementary drug to improve the benefit of DAPT.

Eicosanoids play critical roles in gastric physiology [17]. In GI tract, they mainly function in site of their production, so mucosal tissue was harvested for lipidomic analysis. Presently, we found consistent increase of COX-derived PGs (PGE<sub>2</sub>, PGD<sub>2</sub>, their downstream metabolites and stable form of PGI<sub>2</sub>) in gastric mucosa after adding PQS to DAPT. Notably, PQS supplementation elevated gastric PGE<sub>2</sub> levels more than 20-fold relative to DAPT. ASA-induced gastric injury is primarily due to inhibition of COX activity, resulting in reduced synthesis of mucosal PGs [54]. PGs are crucial mediators for gastroprotection. Almost all of the mucosal defense mechanisms are stimulated or facilitated by PGs, including stimulating mucus secretion, increasing blood flow, accelerating epithelial restitution and mucosal healing [55]. Specifically, PGE<sub>2</sub> administration was reported to attenuate gastric mucosal damage induced by DAPT in rats (unpublished result). Therefore, the gastroprotective effect of PQS on DAPT-induced gastric injury could be partially attributed to the elevated PGs synthesis in gastric mucosa.

The present study evidenced synergistic antiplatelet effect and gastroprotective action by combining PQS with DAPT in AMI rats, which were associated with regulation of eicosanoids metabolism. Some limitations remain. Ginsenosides, the bioactive constituents of PQS, belong to terpenoids class. Phytochemicals in herbal medicine, including terpenoids, are found to broadly change the metabolic patterns of oxylipins by influencing enzymes activity [56], which may explain the lipidomic alterations in current study. Cellular targets and molecular mechanisms underlying the joint effect remain to be elucidated. On the other hand, as platelets are crucial in thrombosis and hemostasis, whether adding PQS to DAPT prolongs bleeding time will be explored in the future.

## Conclusions

In summary, cotreatment with PQS and DAPT achieved better antiplatelet effect attributed to up-regulating AA/PGI<sub>2</sub>, AA/EET synthesis and down-regulating AA/TXA<sub>2</sub> metabolism. PQS mitigated DAPT-induced gastric mucosa injury via promoting mucosal PG production. PQS may provide incremental benefits as a complementary agent to DAPT in the treatment of ACS.

## Abbreviations

DAPT	Dual antiplatelet therapy
ASA	Aspirin
CLP	Clopidogrel
ACS	Acute coronary syndromes
MI	Myocardial infarction
GI	Gastrointestinal
PQ	<i>Panax quinquefolius</i>
PQS	<i>Panax quinquefolius</i> Saponins
HUVEC	Human umbilical vein endothelial cell
AA	Arachidonic acid
COX	Cyclooxygenase
LOX	Lipoxygenase
CYP	Cytochrome P450
PG	Prostaglandin
ADP	Adenosine diphosphate
TTC	2,3,5-Triphenyltetrazolium chloride
AMI	Acute myocardial infarction
TX	Thromboxane
LT	Leukotriene
HETE	Hydroxyeicosatetraenoic acid
LC-MS	Liquid chromatography-mass spectrometer
LAD	Left anterior descending
H&E	Hematoxylin and eosin
PRP	Platelet-rich plasma
PPP	Platelet-poor plasma
LV	Left ventricle
SEM	Scanning electron microscope
PCA	Principal component analysis
OPLS-DA	Orthogonal projection to latent structure-discriminant analysis
VIP	Variable importance in projection
MPAR	Maximal platelet aggregation rate
EET	Epoxyeicosatrienoic acid
DHET	Dihydroxyeicosatrienoic acid
TX	Thromboxane
PPI	Proton pump inhibitor

## Supplementary Information

The online version contains supplementary material available at <https://doi.org/10.1186/s12906-023-04112-7>.

**Additional file 1.** Supplementary materials.

## Acknowledgements

We are grateful for lipidomic technical assistance from Shimadzu (China) Co., LTD Beijing Branch, Beijing, China.

## Authors' contributions

Wenting Wang: Performed the experiments, Conception and design, Data curation, Formal analysis, Writing - original draft. Lei Song: Data curation, Formal analysis, Writing - original draft. Lin Yang: Data curation, Formal analysis, Methodology. Changkun Li: Formal analysis, Methodology. Yan Ma: Supervision, Validation. Mei Xue: Conception and design, Writing - review & editing. Dazhuo Shi: Conception and design, Writing - review & editing.

## Funding

This work was supported by Scientific and technological innovation project of China Academy of Chinese Medical Sciences (CI2021A00913), Innovation Team and Talents Cultivation Program of National Administration of Traditional Chinese Medicine (No: ZYYCXTD-C-202007), Natural Science Foundation of Zhejiang Province (LQ21H290001), National Natural Science Foundation of China (No. 81803949), International Sci-Technology Cooperation Project of China Academy of Chinese Medical Sciences (GH2017-03-05).

## Availability of data and materials

The datasets used and/or analysed during the current study are available from the corresponding author on reasonable request.

## Declarations

### Ethics approval and consent to participate

All animal protocols were reviewed and approved by institutional Ethics Committee of Xiyuan Hospital, China Academy of Chinese Medical Sciences. All methods were carried out in accordance with the National Institutes of Health guide for the care and use of laboratory animals and the guidance on ethical treatment of experimental animals issued by Ministry of Science and Technology of the People's Republic of China. The study was carried out in compliance with the ARRIVE guidelines.

### Consent for publication

Not applicable.

### Competing interests

The authors declare no competing interests.

### Author details

<sup>1</sup>National Clinical Research Center for Chinese Medicine Cardiology, Xiyuan Hospital, China Academy of Chinese Medical Sciences, Beijing 100091, China. <sup>2</sup>Affiliated Hangzhou Chest Hospital, Zhejiang University School of Medicine, Hangzhou 310003, China. <sup>3</sup>Center of Cardiovascular Disease, Xiyuan Hospital, China Academy of Chinese Medical Sciences, Beijing 100091, China. <sup>4</sup>Shimadzu (China) Co., LTD Beijing Branch, Beijing 100020, China. <sup>5</sup>Department of Pathophysiology and Allergy Research, Center of Pathophysiology, Infectiology & Immunology, Vienna General Hospital, Medical University of Vienna, 1090 Vienna, Austria.

Received: 15 October 2022 Accepted: 1 August 2023

Published online: 18 August 2023

## References

- Ibanez B, James S, Agewall S, Antunes MJ, Bucciarelli-Ducci C, Bueno H, Caforio ALP, Crea F, Goudevenos JA, Halvorsen S, Hindricks G, Kastrati A, Lenzen MJ, Prescott E, Roffi M, Valgimigli M, Varenhorst C, Vranckx P, Widimský P. ESC Guidelines for the management of acute myocardial infarction in patients presenting with ST-segment elevation: The Task Force for the management of acute myocardial infarction in patients presenting with ST-segment elevation of the European Society of Cardiology (ESC). *Eur Heart J*. 2017;39(2018):119–77. <https://doi.org/10.1093/eurheartj/ehx393>.
- Petersen AA, Arnesen H, Seljeflot I. A brief review on high on-aspirin residual platelet reactivity. *Vascu Pharmacol*. 2015;67–69:6–9. <https://doi.org/10.1016/j.vph.2015.03.018>.
- Angiolillo DJ, Fernandez-Ortiz A, Bernardo E, Alfonso F, Macaya C, Bass TA, Costa MA. Variability in individual responsiveness to clopidogrel: clinical implications, management, and future perspectives. *J Am Coll Cardiol*. 2007;49:1505–16. <https://doi.org/10.1016/j.jacc.2006.11.044>.
- Bonello L, Tantry US, Marcucci R, Blindt R, Angiolillo DJ, Becker R, Bhatt DL, Cattaneo M, Collet JP, Cuisset T, Gachet C, Montalescot G, Jennings LK, Kereiakes D, Sibbing D, Trenk D, van Werkum JW, Paganelli F, Price MJ, Waksman R, Gurbel PA. Consensus and future directions on the definition of high on-treatment platelet reactivity to adenosine diphosphate. *J Am Coll Cardiol*. 2010;56:919–33. <https://doi.org/10.1016/j.jacc.2010.04.047>.

5. Gurbel PA, Bliden KP, Guyer K, Cho PW, Zaman KA, Kreutz RP, Bassi AK, Tantry US. Platelet reactivity in patients and recurrent events post-stenting: results of the PREPARE POST-STENTING Study. *J Am Coll Cardiol*. 2005;46:1820–6. <https://doi.org/10.1016/j.jacc.2005.07.041>.
6. Adatia K, Farag MF, Gue YX, Srinivasan M, Gorog DA. Relationship of platelet reactivity and inflammatory markers to recurrent adverse events in patients with ST-elevation myocardial infarction. *Thromb Haemost*. 2019;119:1785–94. <https://doi.org/10.1055/s-0039-1695007>.
7. Lanas A, Gargallo CJ. Management of low-dose aspirin and clopidogrel in clinical practice: a gastrointestinal perspective. *J Gastroenterol*. 2015;50:626–37. <https://doi.org/10.1007/s00535-015-1038-3>.
8. Eikelboom JW, Mehta SR, Anand SS, Xie C, Fox KAA, Yusuf S. Adverse impact of bleeding on prognosis in patients with acute coronary syndromes. *Circulation*. 2006;114:774–82. <https://doi.org/10.1161/CIRCULATIONAHA.106.612812>.
9. Bhatt DL, Scheiman J, Abraham NS, Antman EM, Chan FKL, Furberg CD, Johnson DA, Mahaffey KW, Quigley EM. ACCF/ACG/AHA 2008 expert consensus document on reducing the gastrointestinal risks of antiplatelet therapy and NSAID use: a report of the American College of Cardiology Foundation Task Force on Clinical Expert Consensus Documents. *Circulation*. 2008;118:1894–909. <https://doi.org/10.1161/CIRCULATIONAHA.108.191087>.
10. Karmazyn M, Moey M, Gan XT. Therapeutic potential of ginseng in the management of cardiovascular disorders. *Drugs*. 2011;71:1989–2008. <https://doi.org/10.2165/11594300-000000000-00000>.
11. Xue M, Yang L, Shi D, Radauer C, Breiteneder H, Ma Y. Qualitative analysis of xinyue capsules by high-performance liquid chromatography: preliminary evaluation of drug quality in a Sino-Austrian joint study. *Chin J Integr Med*. 2015;21:772–7. <https://doi.org/10.1007/s11655-015-2311-2>.
12. Wang M-M, Xue M, Miao Y, Kou N, Xu Y-G, Yang L, Zhang Y, Shi D. Panax quinquefolium saponin combined with dual antiplatelet drugs inhibits platelet adhesion to injured HUVECs via PI3K/AKT and COX pathways. *J Ethnopharmacol*. 2016;192:10–9. <https://doi.org/10.1016/j.jep.2016.07.015>.
13. Ruggeri ZM. Platelets in atherothrombosis. *Nat Med*. 2002;8:1227–34. <https://doi.org/10.1038/nm1102-1227>.
14. Kou N, Xue M, Yang L, Zang M-X, Qu H, Wang M-M, Miao Y, Yang B, Shi D. Panax quinquefolium saponins combined with dual antiplatelet drug therapy alleviate gastric mucosal injury and thrombogenesis through the COX/PG pathway in a rat model of acute myocardial infarction. *PLoS One*. 2018;13:e0194082. <https://doi.org/10.1371/journal.pone.0194082>.
15. Calder PC. Eicosanoids. *Essays Biochem*. 2020;64:423–41. <https://doi.org/10.1042/EBC20190083>.
16. Yeung J, Hawley M, Holinstat M. The expansive role of oxylipins on platelet biology. *J Mol Med (Berl)*. 2017;95:575–88. <https://doi.org/10.1007/s00109-017-1542-4>.
17. Atay S, Tarnawski AS, Dubois A. Eicosanoids and the stomach. *Prostaglandins Other Lipid Mediat*. 2000;61:105–24. [https://doi.org/10.1016/S0090-6980\(00\)00067-8](https://doi.org/10.1016/S0090-6980(00)00067-8).
18. Wallace JL. Prostaglandins, NSAIDs, and gastric mucosal protection: why doesn't the stomach digest itself? *Physiol Rev*. 2008;88:1547–65. <https://doi.org/10.1152/physrev.00004.2008>.
19. Braune S, Küpper J-H, Jung F. Effect of prostanoids on human platelet function: an overview. *Int J Mol Sci*. 2020;21(23):9020. <https://doi.org/10.3390/ijms21239020>.
20. Kaddurah-Daouk R, Weinshilboum RM. Pharmacometabolomics: implications for clinical pharmacology and systems pharmacology. *Clin Pharmacol Ther*. 2014;95:154–67. <https://doi.org/10.1038/clpt.2013.217>.
21. Krishnamurthy P, Subramanian V, Singh M, Singh K. Deficiency of beta1 integrins results in increased myocardial dysfunction after myocardial infarction. *Heart*. 2006;92:1309–15. <https://doi.org/10.1136/hrt.2005.071001>.
22. Belcher A, Zulfiker AHM, Li OQ, Yue H, Gupta AS, Li W. Targeting thymidine phosphorylase with tipiracil hydrochloride attenuates thrombosis without increasing risk of bleeding in mice. *Arterioscler Thromb Vasc Biol*. 2021;41:668–82. <https://doi.org/10.1161/ATVBAHA.120.315109>.
23. Narverud I, Bogsrud MP, Øyri LKL, Ulven SM, Retterstøl K, Ueland T, Mulder M, van RoetersLennep J, Halvorsen B, Aukrust P, Veierød MB, Holven KB. Lipoprotein(a) concentration is associated with plasma arachidonic acid in subjects with familial hypercholesterolaemia. *Br J Nutr*. 2019;122:790–9. <https://doi.org/10.1017/S0007114519001600>.
24. Kawai T, Yamagishi T, Goto S. Circadian variations of gastrointestinal mucosal damage detected with transnasal endoscopy in apparently healthy subjects treated with low-dose aspirin (ASA) for a short period. *J Atheroscler Thromb*. 2009;16:155–63. <https://doi.org/10.5551/jat.e615>.
25. Gargiulo G, Esposito G, Avvedimento M, Nagler M, Minuz P, Campo G, Gragnano F, Manavifar N, Piccolo R, Tebaldi M, Cirillo P, Hunziker L, Vranckx P, Leonardi S, Heg D, Windecker S, Valgimigli M. Cangrelor, tirofiban, and chewed or standard prasugrel regimens in patients with st-segment-elevation myocardial infarction: primary results of the FABOLUS-FASTER trial. *Circulation*. 2020;142:441–54. <https://doi.org/10.1161/CIRCULATIONAHA.120.046928>.
26. Ye J, Lu S, Wang M, Ge W, Liu H, Qi Y, Fu J, Zhang Q, Zhang B, Sun G, Sun X. Hydroxysafflor yellow A protects against myocardial ischemia/reperfusion injury via suppressing NLRP3 inflammasome and activating autophagy. *Front Pharmacol*. 2020;11:1170. <https://doi.org/10.3389/fphar.2020.01170>.
27. Wang D, Sun X, Yan J, Ren B, Cao B, Lu Q, Liu Y, Zeng J, Huang N, Xie Q, Gu H, Wang J. Alterations of eicosanoids and related mediators in patients with schizophrenia. *J Psychiatr Res*. 2018;102:168–78. <https://doi.org/10.1016/j.jpsychires.2018.04.002>.
28. Yamada M, Kita Y, Kohira T, Yoshida K, Hamano F, Tokuoka SM, Shimizu T. A comprehensive quantification method for eicosanoids and related compounds by using liquid chromatography/mass spectrometry with high speed continuous ionization polarity switching. *J Chromatogr B Analyt Technol Biomed Life Sci*. 2015;995–996:74–84. <https://doi.org/10.1016/j.jchromb.2015.05.015>.
29. Ellero-Simatos S, Beitelshes AL, Lewis JP, Yerges-Armstrong LM, Georgiades A, Dane A, Harms AC, Strassburg K, Guled F, Hendriks MMWB, Horenstein RB, Shuldiner AR, Hankemeier T, Kaddurah-Daouk R. Oxylipid profile of low-dose aspirin exposure: a pharmacometabolomics study. *J Am Heart Assoc*. 2015;4:e002203. <https://doi.org/10.1161/JAHA.115.002203>.
30. Chatterjee M, Ehrenberg A, Toska LM, Metz LM, Klier M, Krueger I, Reusswig F, Elvers M. Molecular drivers of platelet activation: unraveling novel targets for anti-thrombotic and anti-thrombo-inflammatory therapy. *Int J Mol Sci*. 2020;21(21):7906. <https://doi.org/10.3390/ijms21217906>.
31. Alkhamis TM, Beissinger RL, Chediak JR. Artificial surface effect on red blood cells and platelets in laminar shear flow. *Blood*. 1990;75:1568–75.
32. Gawaz M. Role of platelets in coronary thrombosis and reperfusion of ischemic myocardium. *Cardiovasc Res*. 2004;61:498–511. <https://doi.org/10.1016/j.cardiores.2003.11.036>.
33. Wolfe MM, Lichtenstein DR, Singh G. Gastrointestinal toxicity of nonsteroidal antiinflammatory drugs. *N Engl J Med*. 1999;340:1888–99. <https://doi.org/10.1056/NEJM199906173402407>.
34. Dennis EA, Norris PC. Eicosanoid storm in infection and inflammation. *Nat Rev Immunol*. 2015;15:511–23. <https://doi.org/10.1038/nri3859>.
35. Verdoia M, Schaffer A, Barbieri L, Cassetti E, Piccolo R, Galasso G, Marino P, Sinigaglia F, de Luca G. Benefits from new ADP antagonists as compared with clopidogrel in patients with stable angina or acute coronary syndrome undergoing invasive management: a meta-analysis of randomized trials. *J Cardiovasc Pharmacol*. 2014;63:339–50. <https://doi.org/10.1097/FJC.000000000000052>.
36. Verdoia M, Nardin M, Gioscia R, Negro F, Marcolongo M, Suryapranata H, Kedhi E, de Luca G. Higher neutrophil-to-lymphocyte ratio (NLR) increases the risk of suboptimal platelet inhibition and major cardiovascular ischemic events among ACS patients receiving dual antiplatelet therapy with ticagrelor. *Vasc Pharmacol*. 2020;132:106765. <https://doi.org/10.1016/j.vph.2020.106765>.
37. Wu Y, Guo HB, Wang TJ, Wang YY. Comparative study on effects of active ingredients of several traditional Chinese medicines on rabbit platelet aggregation in vitro. *Chin J Clin Pharm Ther*. 2007;12:1047–51.
38. Cameron SJ, Ture SK, Mickelsen D, Chakrabarti E, Modjeski KL, McNitt S, Seaberry M, Field DJ, Le N-T, Abe J-I, Morrell CN. Platelet extracellular regulated protein kinase 5 is a redox switch and triggers maladaptive platelet responses and myocardial infarct expansion. *Circulation*. 2015;132:47–58. <https://doi.org/10.1161/CIRCULATIONAHA.115.015656>.
39. Guo M, Wang P, Du J, Fu C, Yang Q, Gao Z, Zhu M, Lv S, Deng Y, Li T, Shi D, Working Group, For The Xy. Xinyue Capsule in patients with stable coronary artery disease after percutaneous coronary intervention: a multicenter, randomized, placebo-controlled trial. *Pharmacol Res*. 2020;158:104883. <https://doi.org/10.1016/j.phrs.2020.104883>.
40. Quehenberger O, Dennis EA. The human plasma lipidome. *N Engl J Med*. 2011;365:1812–23. <https://doi.org/10.1056/NEJMr1104901>.

41. Bestard-Escalas J, Maimó-Barceló A, Pérez-Romero K, Lopez DH, Barceló-Coblijn G. Ins and outs of interpreting lipidomic results. *J Mol Biol*. 2019;431:5039–62. <https://doi.org/10.1016/j.jmb.2019.08.006>.
42. Imig JD. Eicosanoid blood vessel regulation in physiological and pathological states. *Clin Sci (Lond)*. 2020;134:2707–27. <https://doi.org/10.1042/CS20191209>.
43. Tacconelli S, Patrignani P. Inside epoxyeicosatrienoic acids and cardiovascular disease. *Front Pharmacol*. 2014;5:239. <https://doi.org/10.3389/fphar.2014.00239>.
44. Krötz F, Riexinger T, Buerkle MA, Nithipatikom K, Gloe T, Sohn H-Y, Campbell WB, Pohl U. Membrane-potential-dependent inhibition of platelet adhesion to endothelial cells by epoxyeicosatrienoic acids. *Arterioscler Thromb Vasc Biol*. 2004;24:595–600. <https://doi.org/10.1161/01.ATV.0000116219.09040.8c>.
45. Patrono C, García Rodríguez LA, Landolfi R, Baigent C. Low-dose aspirin for the prevention of atherothrombosis. *N Engl J Med*. 2005;353:2373–83. <https://doi.org/10.1056/NEJMra052717>.
46. Eikelboom JW, Hankey GJ, Thom J, Bhatt DL, Steg PG, Montalescot G, Johnston SC, Steinhubl SR, Mak K-H, Easton JD, Hamm C, Hu T, Fox KAA, Topol EJ. Incomplete inhibition of thromboxane biosynthesis by acetylsalicylic acid: determinants and effect on cardiovascular risk. *Circulation*. 2008;118:1705–12. <https://doi.org/10.1161/CIRCULATIONAHA.108.768283>.
47. Fitzpatrick FA, Ennis MD, Baze ME, Wynalda MA, McGee JE, Liggett WF. Inhibition of cyclooxygenase activity and platelet aggregation by epoxyeicosatrienoic acids. Influence of stereochemistry. *J Biol Chem*. 1986;261:15334–8.
48. Yeomans ND, Lanas AI, Talley NJ, Thomson ABR, Daneshjoo R, Eriksson B, Appelman-Eszczuk S, Långström G, Naesdal J, Serrano P, Singh M, Skelly MM, Hawkey CJ. Prevalence and incidence of gastroduodenal ulcers during treatment with vascular protective doses of aspirin. *Aliment Pharmacol Ther*. 2005;22:795–801. <https://doi.org/10.1111/j.1365-2036.2005.02649.x>.
49. Bittl JA, Laine L. Gastrointestinal injury caused by aspirin or clopidogrel monotherapy versus dual antiplatelet therapy. *J Am Coll Cardiol*. 2021. <https://doi.org/10.1016/j.jacc.2021.10.027>.
50. Uotani T, Sugimoto M, Nishino M, Kodaira C, Yamade M, Sahara S, Yamada T, Osawa S, Sugimoto K, Tanaka T, Umemura K, Watanabe H, Miyajima H, Furuta T. Ability of rabeprazole to prevent gastric mucosal damage from clopidogrel and low doses of aspirin depends on CYP2C19 genotype. *Clin Gastroenterol Hepatol*. 2012;10:879–885.e2. <https://doi.org/10.1016/j.cgh.2012.04.016>.
51. Hallas J, Dall M, Andries A, Andersen BS, Aalykke C, Hansen JM, Andersen M, Lassen AT. Use of single and combined antithrombotic therapy and risk of serious upper gastrointestinal bleeding: population based case-control study. *BMJ*. 2006;333:726. <https://doi.org/10.1136/bmj.38947.697558.AE>.
52. Collet J-P, Thiele H, Barbato E, Barthélémy O, Bauersachs J, Bhatt DL, Dendale P, Dorobantu M, Edvardsen T, Folliguet T, Gale CP, Gilard M, Jobs A, Jüni P, Lambrinou E, Lewis BS, Mehilli J, Meliga E, Merkely B, Mueller C, Roffi M, Rutten FH, Sibbing D, Siontis GCM. ESC Guidelines for the management of acute coronary syndromes in patients presenting without persistent ST-segment elevation. *Eur Heart J*. 2020;42(2021):1289–367. <https://doi.org/10.1093/eurheartj/ehaa575>.
53. Würtz M, Grove EL. Proton pump inhibitors in cardiovascular disease: drug interactions with antiplatelet drugs. *Adv Exp Med Biol*. 2017;906:325–50. [https://doi.org/10.1007/5584\\_2016\\_124](https://doi.org/10.1007/5584_2016_124).
54. Wallace JL. Nonsteroidal anti-inflammatory drugs and gastroenteropathy: the second hundred years. *Gastroenterology*. 1997;112:1000–16. <https://doi.org/10.1053/gast.1997.v112.pm9041264>.
55. Laine L, Takeuchi K, Tarnawski A. Gastric mucosal defense and cytoprotection: bench to bedside. *Gastroenterology*. 2008;135:41–60. <https://doi.org/10.1053/j.gastro.2008.05.030>.
56. Gladine C, Ostermann AI, Newman JW, Schebb NH. MS-based targeted metabolomics of eicosanoids and other oxylipins: analytical and inter-individual variabilities. *Free Radic Biol Med*. 2019;144:72–89. <https://doi.org/10.1016/j.freeradbiomed.2019.05.012>.

## Publisher's Note

Springer Nature remains neutral with regard to jurisdictional claims in published maps and institutional affiliations.

Ready to submit your research? Choose BMC and benefit from:

- fast, convenient online submission
- thorough peer review by experienced researchers in your field
- rapid publication on acceptance
- support for research data, including large and complex data types
- gold Open Access which fosters wider collaboration and increased citations
- maximum visibility for your research: over 100M website views per year

At BMC, research is always in progress.

Learn more [biomedcentral.com/submissions](https://biomedcentral.com/submissions)

